Journal of Non-Crystalline Solids xxx (xxxx) xxx–xxx

Contents lists available at ScienceDirect

Journal of Non-Crystalline Solids

journal homepage: www.elsevier.com/locate/jnoncrysol

Nano-heterogeneity of natural impact silica-rich glasses according to atomic force microscopy and spectroscopy data

Yevgeny A. Golubev[a,*], Tatyana G. Shumilova[a,b], Sergey I. Isaenko[a], Boris A. Makeev[a], Alexandr A. Utkin[c], Elena I. Suvorova[d], Kord Ernstson[e]

[a] Institute of Geology of Komi SC of Uralian Branch of RAS, 54 Pervomayskaya st., Syktyvkar 167982, Russia
[b] Hawaii Institute of Geophysics and Planetology, University of Hawaii at Manoa, 1680 East-West Road, Honolulu, HI 96822, USA
[c] Department of Radiophysics, Syktyvkar State University, 55, Oktyabrsky st., Syktyvkar 167000, Russia
[d] Institute of Crystallography of RAS, 59 Leninsky pr., Moscow 117333, Russia
[e] Faculty of Philosophy I, University of Würzburg, Germany

ARTICLE INFO

Keywords:
Natural silica-rich glasses
Microscopy
Spectroscopy
Surface nano-heterogeneity

ABSTRACT

In nature extreme PT-conditions result in numerous glass-like solids, the study of which allows specifying various structural and chemical features of extreme materials, which have a great application potential in various fields of technology. We studied features of nanostructure of natural impact glasses, including recently discovered ultrahigh-pressure high-temperature impact glasses, compared to low-pressure natural and synthetic standard silica glasses. In this paper we presented complex data of atomic force microscopy, X-ray diffraction, X-ray energy-dispersive spectrometry, infrared and Raman spectroscopy. We described nanostructural characteristics of impact glasses and showed influence of chemical composition on the features of their structure. We discovered that the elemental composition was the most important factor determining the glasses nano-heterogeneity. We noted an essential role of influence of Na impurity on glass nanostructure. The impact glasses with pure SiO_2 composition have the smallest sizes of nanostructural elements.

1. Introduction

Despite a wide application of glasses and a long history of their study, there is still no generally accepted understanding and definition of the state of this type of substance. Often, any solid amorphous substance is referred to as glass [1–5]. In this paper we use a classical definition [5]. We refer to the term “glass” as substance formed at a rapid solidification of the melt near the glass transition temperature, when the cooling velocity exceeds the maximum for crystallization under these PT-conditions [6–8].

In geological environment glass is formed as a result of the following processes:

(i) Meteorite impact glass, as a result of falling large asteroids, leading to melting of target rocks at ultrahigh pressures (35–90 GPa) and temperatures (up to 3000 °C and higher) [9–12], followed by rapid cooling and formation – a) *proximal impactites*, rocks with a high content of condensed impact melt, including glasses; b) distal emissions in the form of *bombs* and *tektites* deposited from a dust cloud over large areas outside craters [6,10,13–18]; c) *ultrahigh-pressure melt impactites of vein type*, forming dikes penetrating impactites of the 1st generation, which were first discovered on the territory of the Kara astrobleme [19].
(ii) Volcanic glass – *pumice*, *obsidian*, from condensation of silica-rich magmatic melts on the earth's surface.
(iii) *Tachylite*, a black volcanic glass, which is formed by the chilling of basaltic magmas.
(iv) *Pseudotachylite*, a mostly devitrified glass, which may form via frictional melting of faults, in large-scale landslides, and by impact processes.
(v) *Buchite*, from pyrometamorphism at the contact of acid rocks with intrusion magma of basic composition, leading to partial melting of the enclosing rocks.
(vi) *Fulgurites*, melting of rocks when lightning strikes the ground [20–23].

Impact glasses forming from ultrahigh-pressure high-temperature exposure to target rocks are the most interesting due to their potentially unusual properties. These glasses can be used to solve fundamental problems of the state of substance under extreme conditions and to

* Corresponding author.
E-mail addresses: yevgenygolubev74@mail.ru, golubev@geo.komisc.ru (Y.A. Golubev).

https://doi.org/10.1016/j.jnoncrysol.2018.08.031
Received 11 June 2018; Received in revised form 14 August 2018; Accepted 23 August 2018

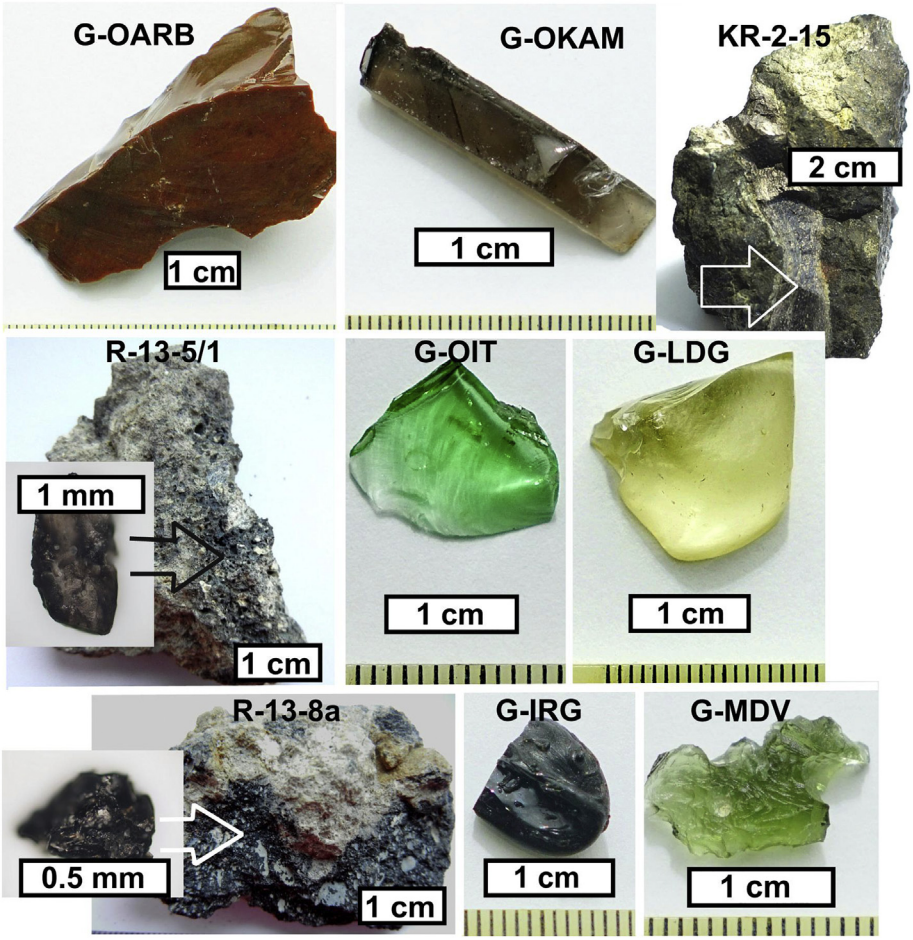

Fig. 1. Photos of studied glasses.

Table 1
Short description of the glass samples.

Sample code	Name	Origin, locality	Initial origin features	Color	Optical transparence
KR-2-15	UHPHT impact glass	Vein body within suevite, Kara astrobleme, Pay-Khoy (river Kara, left bank), sampled by T.G.Shumilova in 2015 year	UHPHT	Gray	Translucent
R-13-5/1	Impact glass	Glass drops from suevites, Ries crater, Altenburg quarry, Germany, sampled by T.G.Shumilova and K.Ernstson in 2013 year	HPHT	Gray	Translucent
R-13-8a	Impact glass	Glass drops from suevites, crater Ries, Polsingen quarry, Germany, sampled by T.G.Shumilova and K.Ernstson in 2013 year	HPHT	Gray	Translucent
G-MDV	Moldavite	Tektite, Bohemia (impact origin, probable Ries (Germany) impact distal ejecta), from N.P.Yushkin's collection	HPHT	Green	Translucent
G-IRG	Irgizite	Tektite from Zhamanshin outer crater deposits, Kazakhstan, from N.P.Yushkin's collection	HPHT	Black	Opaque
G-LDG	Libyan desert glass	Probable meteoritic origin, Egypt, from N.P.Yushkin's collection	HPHT	Yellow	Translucent
G-OKAM	Obsidian	Volcanic glass, Paratunskoye deposit, Kamchatka, from N.P.Yushkin'scollection	LPHT	Dark brown	Opaque
G-OARB	Obsidian	Volcanic glass, volcanic cone Arteny, Armenia, from N.P.Yushkin's collection	LPHT	Dark brown	Opaque
G-OIT	Obsidian	Volcanic glass, Sardinia island, Italy, from N.P.Yushkin's collection	LPHT	Green	Translucent
Suprasil	Standard quartz glass	Manufactured glass, Bruker, Germany	LPHT	Colorless	Translucent

Subscription: UHPHT – ultrahigh pressure high temperature; HPHT – high pressure high temperature; LPHT – low pressure (ambient pressure) high temperature.

create fundamentally new materials [24–28].

Differences in concentration and composition of impurities and PT-condensation conditions for different formation processes contribute to nanoscale chemical heterogeneity in these types of glasses. This heterogeneity was mainly observed by transmission electron microscopy (TEM) [29–31]. In the last two decades, atomic force microscopy (AFM) methods are actively used to study topographic nanoscale heterogeneity of glasses. Although most AFM studies were carried out for artificial glasses [e.g. 33–39], including for the evaluation of phase separation [40], natural glasses were also investigated by these methods [41–44]. The finding of new specific types of natural impact glasses, in particular ultra-high pressure glasses from the Kara astrobleme [19], stimulated interest for further studies of impact glasses, including methodological interpretations, in particular for AFM results. Here, we report on AFM quantitative estimates of nanoscale heterogeneity of the glasses surface considering the sizes of hillocks as

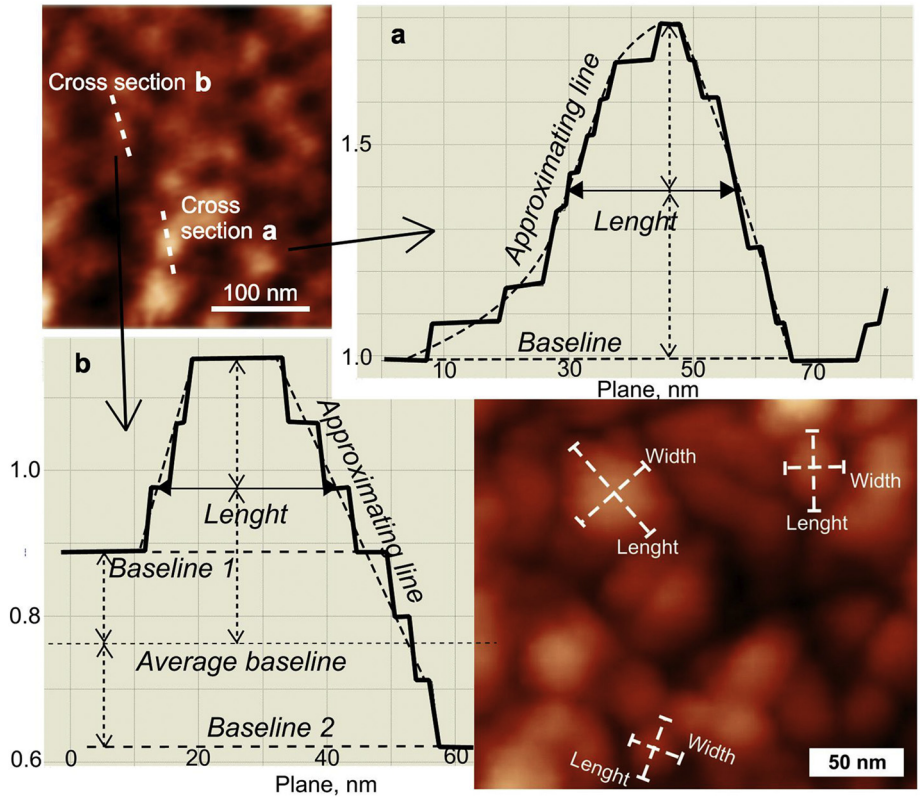

Fig. 2. Scheme of measuring the size of hillocks on an AFM image of a glass surface.

Table 2
Composition of rock-forming oxides in the silicate matrix of the glasses (at.%).

Sample	SiO_2	MgO	Al_2O_3	Na_2O	K_2O	CaO	TiO_2	Fe_2O_3
G-LDG	98.1	–	0.8	–	–	–	0.2	0.3
G-IRG	80.6	3.2	10.0	0.9	1.2	1.4	0.6	3.5
G-MDV	82.8	1.8	9.7	0.4	2.1	1.8	0.3	0.8
G-OKAM	76.5	1.7	3.3	9.8	0.3	4.0	–	0.2
G-OIT	75.8	5.2	1.8	11.1	0.3	7.1	0.2	0.2
G-OARB	71.9	0.2	16.5	3.7	3.7	0.6	0.3	0.5
KR-2-15	71.8	4.0	16.1	5.1	1.6	1.1	0.3	0.5
R-13-5/1	67.6	2.6	16.5	2.7	2.1	3.2	0.6	4.0
R-13-8a	58.0	2.6	14.6	1.6	2.9	2.2	0.9	3.7
Suprasil	99.8	–	–	–	–	–	–	–

The content of the rock-forming oxides in the studied glasses practically coincides with data previously reported in the literature, for example [19,46–49].

proposed in [44], and the paper aims at the comparison of the nanostructure of meteorite impact glasses and natural glasses of different geological origin and the influence of the chemical composition on it.

2. Experimental

2.1. Glass samples

The objects of our study were natural impact glasses of the Kara astrobleme (Pay-Khoy, Russia), represented by the UHP high temperature specimens of the vein type [19], impact glasses from the suevites of the Ries crater (disused Altenbürg and Polsingen quarries, Germany), two samples of tektites – *moldavite* (Czech Republic) and *irgizite* from the Zhamanshin impact crater (Kazakhstan), impact glasses from the desert - *Libyan Desert glass* (Egypt). For comparison, three samples of low-pressure volcanogenic obsidian glasses (Kamchatka Peninsula, Armenia and Italy) were studied (Fig. 1). We used the manufactured quartz glass Suprasil (Bruker) as a standard. Table 1 compiles the studied samples and their origin.

2.2. Samples preparation

The surface of the samples for the study was prepared by cleavage. The sample was a washer a few millimeters in diameter and 2–4 mm in height. It was glued on a metal washer 1 cm in diameter, the cleavage surface was directed upwards. The freshly cleaved surface was subsequently studied by atomic force microscopy and Raman spectroscopy. Then, this surface was covered by a layer of carbon, and the sample was tested by an electron microscope and energy-dispersive spectral analysis. The powdered samples were used for X-ray diffraction analysis and IR spectroscopy.

2.3. Characterization techniques

The surface morphology has been characterized by AFM measurement in tapping mode using an Integra Prima (NT-MDT, Russia) with super sharp silicon cantilevers of model SSS-NCH (Nanosensors). The resonant frequency of cantilevers is about 330 kHz, the radius at the end is 2–4 nm and the stiffness constant is about 35 N/m. The images have been recorded at a scan frequency between 0.8 and 1 Hz for a resolution of 512 × 512 pixels. For each sample we perform at least 25 AFM images with 5–7 different scan areas.

AFM scanning of the glass surface is challenging due to the static electricity, which significantly increases the observed size of the hillocks and reduces the clarity of image. To reduce this effect, the surface of the samples was grounded by a silver paste, and the air in the room was moistened.

The measuring procedure was as follows (Fig. 2). For contacting hillocks along the surface profiles we measured the long and short axes (width and length) of the roughly elliptically shaped objects. Due to the complex surface relief, the bases of the hillocks are usually at different heights. For this reason, the sizes were measured halfway up the

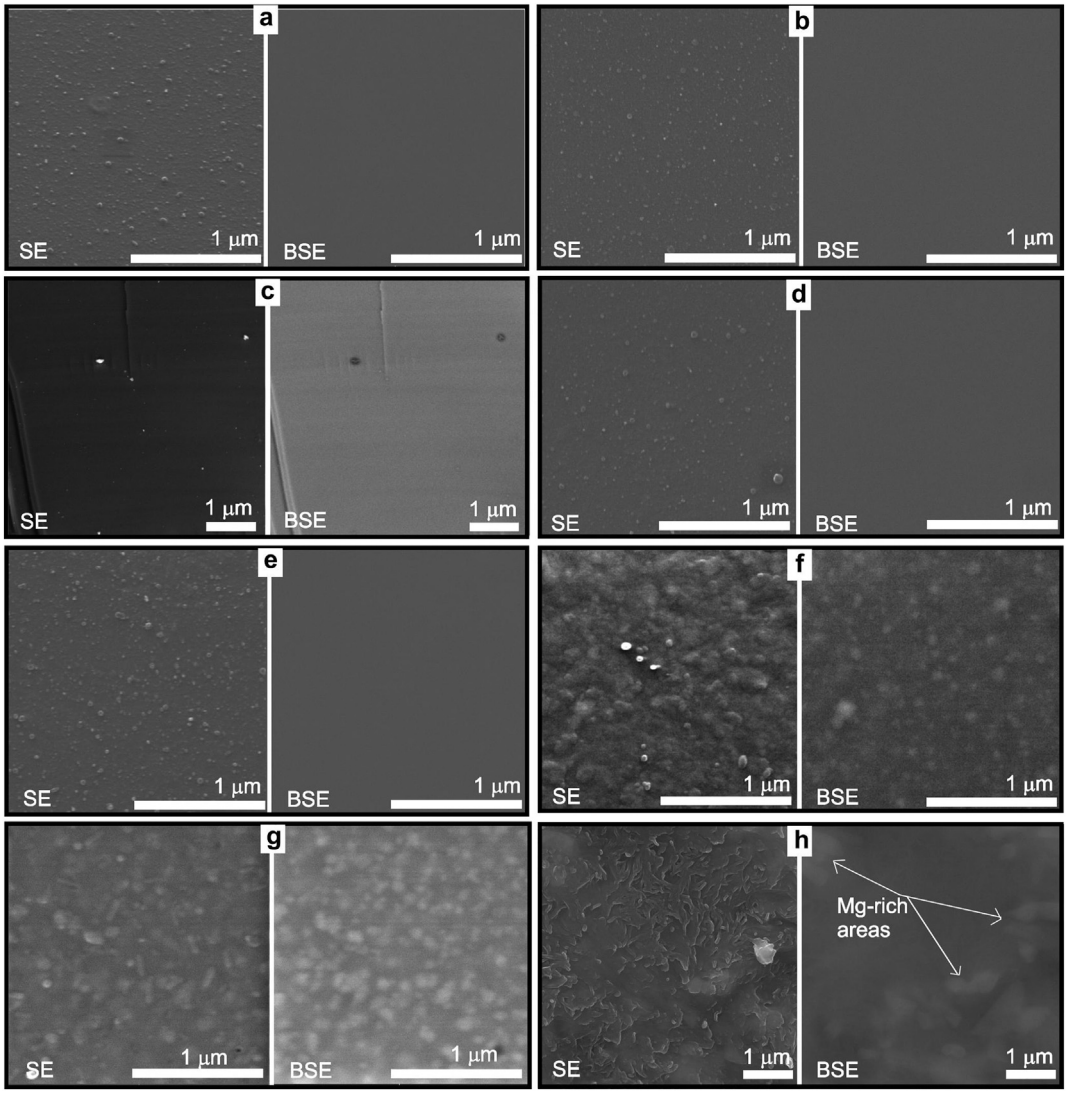

Fig. 3. SEM images (left – in secondary electrons (SE); right – in backscattered electrons (BSE)) of glass surface: a - G-LDG; b - G-MDV; c - G-IRG; d - G-OKAM; e – G-OARB; f - R-13-5/1; g - R-13-8a; h - KR-2-15.

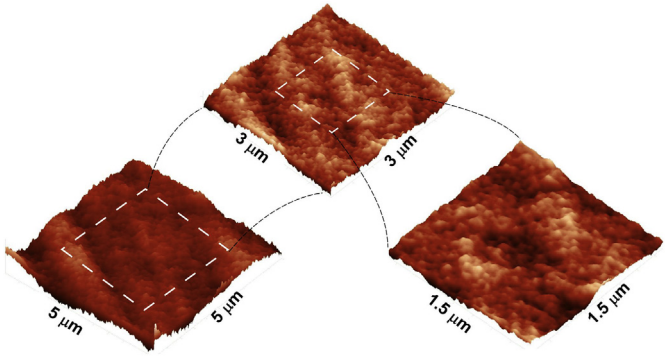

Fig. 4. Typical topography of the fracture surface of natural glass at different magnifications (for irgizite).

hillocks. The height was measured from the average baseline between the baselines of the hillock to the summit. Such an approach allows somehow decreasing the object broadening effect on the surface by a probe. We did not measure the size of the hillocks located above the level of neighboring hillocks, as the distortion of the shape and size of a hillock as a result of convolution with the shape of the AFM needle is very pronounced. The technique was described in detail in [44].

We measured sizes of 95–120 hillocks for various samples. The equation determining the average size for a log-normal distribution and the decimal logarithm of hillock sizes for finding the most likely size (d_m) were used for calculations. The range of sizes for N hillocks from the minimum to the maximum value was divided into equal intervals. The average size of hillocks d_m was calculated by Eq. [45]:

$$d_m = \frac{1}{N}\sum_{1}^{n} q_i \bullet m_i \tag{1}$$

where m_i is the middle of each interval; n is the number of intervals; q_i is the number of hillocks in each interval. To evaluate the hillocks size distribution, the standard deviation s was used by equation:

$$s = \sqrt{\frac{1}{N-1}\sum_{1}^{n} q_i \bullet (m_i - d_m)^2} \tag{2}$$

The cleaved surfaces of the samples were studied with a Tescan MIRA3 scanning electron microscope. X-ray energy-dispersive spectrometry (EDS) with AZTEC software (Oxford Instruments) provided the elemental composition and quantification (in atomic %, averaged for five measurements). The microprobe was operated at an emission current of 100 μA, a specimen current of 100 pA, an accelerating

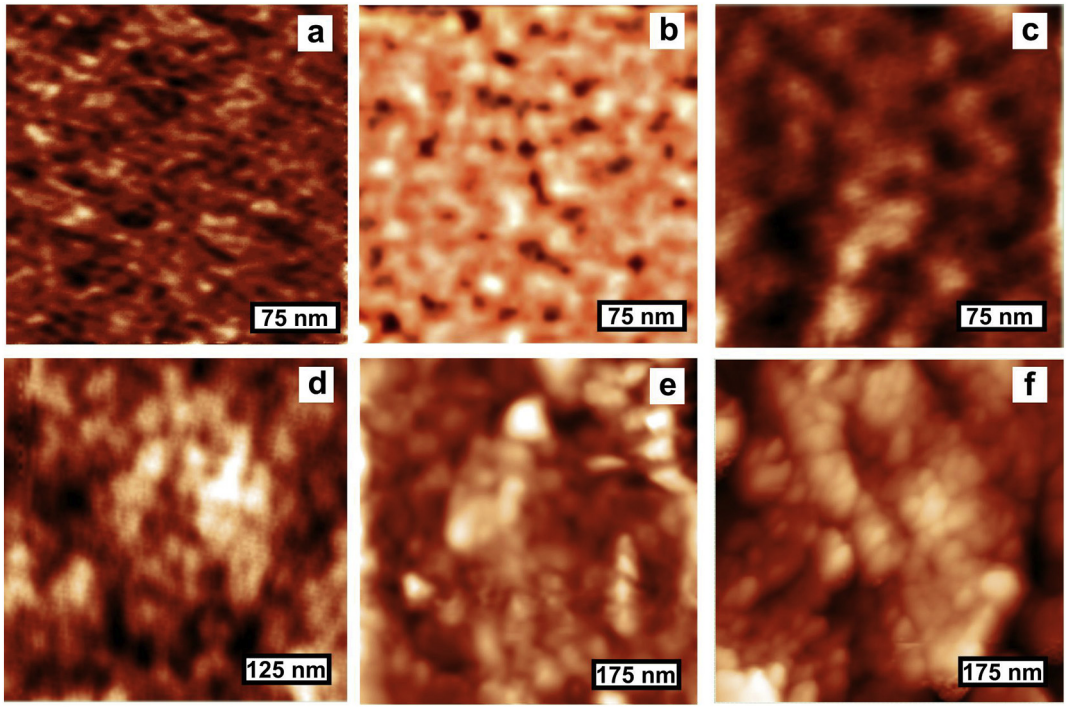

Fig. 5. Characteristic AFM-images of glass fracture surfaces: a – Suprasil; b – Libyan desert glass; c – moldavite; d – obsidian from Kamchatka; e – KP-2-15; f – R-13-5/1.

potential of 20 kV.

Raman spectroscopy was carried out with a LabRam HR800 instrument (Horiba, Jobin Yvon) at room temperature. The system was equipped with an Olympus BX41 optical microscope and a Si-based CCD detector. Spectra were recorded in the 100–4000 cm^{-1} range using a spectrometer grating of 600 g/mm, with a confocal hole size of 300 μm and a slit of 100 μm. The exciting radiation of a He—Ne laser (632.8 nm, 2 mW) was used. After background correction, individual lines were deconvolved with a curve-fitting procedure from the LabSpec 5.36 software.

The atomic structure was studied in a FEI CM300UT FEG transmission electron microscope (300 kV field emission gun, 0.65 mm spherical aberration, and 0.17 nm resolution at Scherzer defocus). The images were recorded on a Gatan-797 slow scan CCD camera with a 1024 × 1024 pixels/14 bit detector. The samples for HRTEM-studies were broken into small pieces. Grains less than 2.0 μm were used for HRTEM. The powdered grains were placed onto carbon films deposited on copper grids. Measurements were made on thin sections with a thickness between 40 and 100 nm at grain edges. The images were processed with the Digital Micrograph software (Gatan).

The XRD examine were carried by using a Shimadzu XRD-6000 diffractometer which was operated at 30 kV and 30 mA, with CuKα (λ = 1·54 Å) radiation and Ni filter, at a scanning speed 0.25° (2θ)/min in the range recorded from 10 to 45° (2θ). Signals were recorded at intervals of 0.05° (2θ). Powder samples were placed onto an aluminum plate.

IR spectra were recorded by Infralyum FT801 FTIR Spectrometer (Lyumex-Siberia Company, Novosibirsk, Russia). All assays were performed in the wavenumber region 4000–500 cm^{-1}. The resolution was 4 cm^{-1}, 32 scans were registered. Thin transparent pellets were made by compacting an intimate mixture obtained by shaking 2 mg of sample in 100 mg of dry KBr.

3. Results

3.1. EDS analysis

The composition of the glass matrix was determined by EDS analysis (Table 2). The silica content among the studied samples increases in sequence: proximal impact condensed melts – volcanic glasses – distal tektites – distal desert impactite, glass standard.

3.2. Microscopy of glasses

SEM images in SE mode show a characteristic surface of a shell-like fracture of a cleavage surface of tektites and volcanic glasses with small hillocks (Fig. 3a-e). Suevite impact glasses have more complicated surface relief (Fig. 3f, h), sample R-13-8a present globules and elongated morphological elements with the diameter of about 80 nm (Fig. 3g). The images in BSE mode show a microscopically homogeneous structure of the glasses (Fig. 3a-e) except samples R-13-5/1, R-13-8a and KR-2-15 (Fig. 3f-h). In this case, the samples of R-13-5/1 and R-13-8a are compositionally homogeneous. Probably, for these samples we observe the influence of the topography of the surface on the images in BSE mode or secondary phase separation similar to those studied by the AFM method in the work [40] on the example of sodium silicate glasses. The bright inner regions on the BSE images in sample KR-2-15 are enriched in magnesium.

In AFM studies, the surface of glasses is usually characterized by the roughness measured in the standard software of any atomic force microscope [33–38]. However, the measurement of surface roughness does not meet the objectives set out in this paper. Roughness is correctly measured only on samples with an almost perfectly flat surface. In this case, the software alignment of distortions, introduced by the scanner, allows a correct estimate of the roughness. Smooth and flat surfaces are obtained with special techniques (polishing, chemical grinding) [50]. Software smoothing applied to distortions by the macrorelief of the cleaved surface of the glass, introduces an error to the measured roughness. Additionally, the manifold possible artifacts can influence the roughness estimate [51].

presence of modifying impurities partially enveloping the nano-sized regions of the glass-forming matrix contributes to the fracture of the material along the impurity-containing regions and to the formation of a roughness on the fracture surface. In relatively pure silica glasses (Suprasil, Libyan desert glass), the nano-roughness of the surface probably reflects statistical fluctuations in the density of glass former in the melt. Thus, the pure SiO_2 drops of UHPHT glasses found within the vein-like bodies of the Kara impact structure [19] may promise a greater homogeneity at nanoscale.

Acknowledgments

The work was supported by Russian Science Foundation (project 17-17-01080). The authors are thankful to Galina N. Lysyuk for provided samples of Libyan desert glass, irgizite and moldavite from N.P.Yushkin's collection, and to *V*ladimir P. Lyutoev for the presented sample of Suprasil, and also to Viktor A. Radaev – for realization of the AFM observations, Marina F. Samotolkova for IR studies. The equipment of the Center for Collective Use "Geoscience" of the Institute of Geology of the Komi SC UB RAS was used for our study.

References

[1] M.M. Shulz, O.V. Mazurin, Modern Concepts about Structure of Glasses and their Properties. Nauka, Leningrad, (1988) (in Russian).
[2] A.F. Skryshevsky, A Structural Analysis of Liquids and Amorphous Bodies. 2nd Prod. Revised. The Higher School, Moscow, (1980).
[3] S. Horst, Glass – Nature, Structure, and Properties, Springer, 1991.
[4] A.C. Wright, Neutron scattering from vitreous silica. V. The structure of vitreous silica: what have we learned from 60 years of diffraction studies? J. Non-Crystalline Solid 179 (1994) 84–115.
[5] C.A. Angell, Formation of glasses from liquids and biopolymers, Science 267 (1995) 1924–1935.
[6] G.S. Henderson, The structure of silicate melts: glass perspective, Can. Mineral. 43 (2005) 1921–1958.
[7] I. Friedman, W. Long, Volcanic glasses, their origins and alteration processes, J. Non-Cryst. Solids 67 (1984) 127–133.
[8] K. Heide, G. Heide, Vitreous state in nature – origin and properties, Chem. Erde 71 (2011) 305–335.
[9] D. Stöffler, F. Langenhorst, Shock metamorphism of quartz in nature and experiment. I. Basic observation and theory, Meteoritics 29 (1994) 155–181.
[10] B.M. French, Traces of catastrophe: a handbook of shock-metamorphic effects in terrestrial meteorite impact structures, LPI Contribution, Vol. 954 Lunar and Planetary Institute, Houston, Texas, 1998.
[11] V.L. Masaitis, M.S. Mashchak, A.I. Raikhlin, G.I. Shafranovsky, T.V. Selivanovskaya, Diamond-Bearing Impactites of 971 the Popigai Astrobleme, VSEGEI, Saint-Petersburg, 1998 in Russian.
[12] F. Langenhorst, Shock metamorphism of some minerals: basic introduction and microstructural observations, Bull. Czech Geol. Surv. 77 (2002) 265–282.
[13] G.T. Skublov, Yu.B. Marin, V.M. Semikolennykh, S.G. Skublov, Yu.N. Tarasenko, Volkhovite – a newtype the tektite-like glasses, Proc. Russ. Mineral. Soc. 136 (2007) 50–68.
[14] R.F. Fudali, M.D. Dyar, D.L. Griscom, H.D. Schreiber, The oxidation state of iron in tektiteglass, Geochim. Cosmochim. Acta 51 (1987) 2749–2756, https://doi.org/10.1016/0016-7037(87)90154-2.
[15] G.S. Henderson, G. Calas, J.F. Stebbins, The structure of silicate glasses and Melts, Elements 2 (2006) 269–273.
[16] H.J. Melosh, Impact Cratering – A Geological Process, Oxford Univ. Press, New York, 1989.
[17] M. Trnka, S. Houzar, Moldavites: a review, Bull. Czech Geol. Surv. 77 (4) (2002) 283–302.
[18] P.J. Heaney, P.J. Heaney (Ed.), Silica, Physical Behavior, Geochemistry and Materials Applications, Mineralogical Society of America, Washington, DC, 1994, pp. 1–39.
[19] T.G. Shumilova, S.I. Isaenko, B.A. Makeev, A.A. Zubov, S.N. Shanina, Y.M. Tropnikov, A.A. Askhabov, Ultrahigh-pressure liquation of an impact melt. Part 1, Doklady Earth Sciences, 480 2018, pp. 595–598.
[20] R. Clocchiatti, Fulgurites and vitreous rocks from Etna - a preliminary petrochemical study, Eur. J. Mineral. 2 (4) (1990) 479–494.
[21] S.J. Desch, W.J. Borucki, C.T. Russell, A. Bar-Nun, Progress in planetary lightning, Rep. Prog. Phys. 65 (2002) 955–997, https://doi.org/10.1088/0034-4885/65/6/202.
[22] A.Yu. Lysyuk, G.A. Yurgenson, N.P. Yushkin, Fitofulgurite – new type the electro-atmogenic geological occurrences, Lithosphere 3 (2006) 125–140 (in Russian).
[23] K. Block, Fulgurite Classification, Petrology, and Implications for Planetary Processes, Master's thesis The University of Arizona, 2011, p. 69.
[24] D. Bolmatov, V.V. Brazhkin, K. Trachenko, Thermodynamic behavior of supercritical matter, Nat. Commun. 4 (2013) 2331, https://doi.org/10.1038/ncomms3391.
[25] P.A. Borisova, M.S. Blanter, V.V. Brazhkin, V.A. Somenkov, V.P. Filonenko, Phase transformations in amorphous fullerite C-60 under high pressure and high temperature, J. Phys. Chem. Solids 83 (2015) 104–108.
[26] M. Guerette, M.R. Ackerson, J. Thomas, F. Yuan, E.B. Watson, D. Walker, L. Huang, Structure and properties of silica glass densified in cold compression and hot compression, Sci. Rep. 5 (2015) 15343, https://doi.org/10.1038/srep15343.
[27] A.Yu. Lysyuk, Petrofulgurites: electro-atmogenic differentiation of substance, Vestnik IG Komi SC UB RAS. 5 (2009) 14–17 in Russian.
[28] V.P. Lyutoev, A.Yu. Lysyuk, Structure and texture of silica of impactites of the kara astrobleme, Vestnik IG Komi SC UB RAS. 9 (2015) 24–32 in Russian.
[29] P.H. Gaskell, Structure and properties of glasses — how far do we need to go? J. Non-Cryst. Solids 222 (1997) 1–12.
[30] N. Terakado, K. Tanaka, Nanoscale heterogeneous structures in GeO2–GeS2 glasses, Jpn. J. Appl. Phys. 47 (2008) 7972.
[31] T.A. Gornostaeva, A.V. Mokhov, P.M. Kartashov, O.A. Bogatikov, Condensate glasses from the Zhamanshin Crater. I. Irghizites, Petrology 24 (1) (2016) 1–20.
[32] T.A. Gornostaeva, A.V. Mokhov, P.M. Kartashov, O.A. Bogatikov, Condensate glasses from the Zhamanshin Crater. II. Zhamanshinites, Petrology 25 (1) (2017) 3–25.
[33] C. Wünsche, E. Rädlein, G.H. Frischat, Glass fracture surfaces seen with an atomic force microscope, Fresenius J. Anal. Chem. 358 (1997) 349–351.
[34] W. Raberg, K. Wandelt, Atomically resolved AFM investigations of an amorphous barium silicate surface, Appl. Phys. A Mater. Sci. Process. 66 (1998) S1143–S1146.
[35] A. Hervé, A. Daniel, Ten years of atomic force microscopy in glass research, Ceramics-Silikáty 44 (4) (2000) 121–128.
[36] J.-F. Poggemann, A. Goβ, G. Heide, E. Rädlein, G.H. Frischat, Direct view of the structure of a silica glass fracture surface, J. Non-Crystal. Solids 281 (2001) 221–226.
[37] W. Raberg, A.H. Ostadrahimi, T. Kayser, K. Wandelt, Atomic scale imaging of amorphous silicate glass surfaces by scanning force microscopy, J. Non-Cryst. Solids 351 (12–13) (2005) 1089–1096.
[38] D. Dalmas, A. Lelarge, D. Vandembroucq, Quantitative AFM analysis of phase separated borosilicate glass surfaces, J. Non-Cryst. Solids 353 (52–54) (2007) 4672–4680.
[39] R.L. Smith, J.J. Mecholsky Jr., Application of atomic force microscopy in determining the fractal dimension of the mirror, mist, and hackle region of silica glass, Mater. Charact. 62 (2011) 457–462.
[40] B.R. Wheaton, A.G. Clare, Evaluation of phase separation in glasses with the use of atomic force microscopy, J. Non-Cryst. Solids 353 (2007) 4767–4778.
[41] E. Radlein, G.H. Frischat, Atomic force microscopy as a tool to correlate nanostructure to properties of glasses, J. Non-Cryst. Solids 222 (1997) 69–82.
[42] G. Heide, B. Muller, G. Kloess, D. Moseler, G.H. Frischat, Structural classification of natural non-crystalline silicates, J. Non-Cryst. Solids 323 (2003) 68–71.
[43] G.H. Frischat, J.-F. Poggemann, G. Heide, Nanostructure and atomic structure of glass seen by atomic force microscopy, J. Non-Cryst. Solids 345 (2004) 197–202.
[44] Ye.A. Golubev, S.I. Isaenko, Scanning probe microscopy in mineralogical studies: about origin of the observed roughness of natural silica-rich glasses, IOP Conf. Ser. 256 (2017) 012019, , https://doi.org/10.1088/1757-899X/256/1/012019.
[45] R. Storm, Probability Theory. Mathematical Statistics. Statistical Quality Control, Mir, Moscow, 1970 (Russian translation).
[46] T. Magna, A. Deutsch, K. Mezger, R. Skála, H.′.M. Seitz, J. Mizera, Z. Canda, L. Adolph, Lithium in tektites and impact glasses: Implications for sources, histories and large impacts, Geochim. Cosmochim. Acta 75 (2011) 2137–2158.
[47] I. Vêtvicka, J. Frank, J. Drtina, Electron microprobe analysis (WDS EPMA) of Zhamanshin glass reveals the impactor and a common role of accretion in the origin of splash form impact glass, IOP Conf. Ser. 7 (1) (2010) 012029.
[48] E. Faulques, E. Fritsch, M. Ostroumov, Spectroscopy of natural silica-rich glasses, J. Mineral. Petrol. Sci. 96 (2001) 120–128.
[49] G. Giuli, E. Paris, G. Pratesi, C. Koeberl, C. Cipriani, Iron oxidation state in the Fe-rich layer and silica matrix of Libyan Desert Glass: a high-resolution XANES study, Meteorit. Planet. Sci. 38 (2003) 1181–1186.
[50] N.P. Mellott, S.L. Brantley, J.P. Hamilton, C.G. Pantano, Evaluation of surface preparation methods for glass, Surf. Interface Anal. 31 (5) (2001) 362–368.
[51] J.M. Bennett, J. Jahanmir, J.C. Podlesny, T.L. Balter, D.T. Hobbs, Scanning force microscope as a tool for studying optical surfaces, Appl. Opt. 34 (1995) 213–218.
[52] I. Liritzis, M. Bonini, N. Laskaris, Obsidian hydration dating by SIMS-SS: surface suitability criteria from atomic force microscopy, Surf. Interface Anal. 40 (2008) 458–463, https://doi.org/10.1002/sia.2672.
[53] C. Marliere, S. Prades, F. C'elari'e, D. Dalmas, D. Bonamy, C. Guillot, E. Bouchaud, Crack fronts and damage in glass at the nanometer scale, J. Phys. 15 (2003) S2377–S2386.
[54] D. Bonamy, S. Prades, C.L. Rountree, L. Ponson, D. Dalmas, E. Bouchaud, K. Ravi-Chandar, C. Guillot, Nanoscale damage during fracture in silica glass, Int. J. Fract. 140 (1–4) (2006) 3–14.
[55] P.F. McMillan, G.H. Wolf, B.T. Poe, Vibrational spectroscopy of silicate liquids and glasses, Chem. Geol. 96 (1992) 351–366.
[56] N.N. Anfilogov, N.N. Bykov, V.N. Osipov, Silicate melts, Nauka, Moscow, 2005 (in Russian).
[57] A. Gucsik, C. Koeberl, F. Brandstätter, E. Libowitzky, M. Zhang, Infrared, Raman, and cathodoluminescence studies of impact glasses, Meteorit. Planet. Sci. 39 (2004) 1273–1285.
[58] N.P. Mellott, C.G. Pantano, A Mechanism of Corrosion-Induced Roughening of Glass Surfaces, Int. J. Appl. Glas. Sci. 4 (3) (2013) 274–279.
[59] G. Pallares, F. Lechenault, M. George, E. Bouchaud, C. Ottina, C.L. Rountree, M. Ciccotti, Roughness of silica glass sub-critical fracture surfaces, Ceram. Trans. 230 (2012) 77–84.

[60] E. Gavars, A. Svagere, A. Skudra, N. Zorina, R. Poplausks, Measurements of SiO2 glass surface parameters by methods of microscopy, IOP Conf. Ser. 38 (1) (2012) 012043.
[61] S.M. Wiederhorn, J.M. López-Cepero, J. Wallace, J.-P. Guin, T. Fett, Roughness of glass surfaces formed by sub-critical crack growth, J. Non-Cryst. Solids 353 (16–17) (2007) 1582–1591.
[62] G.N. Greaves, EXAFS and the structure of glass, J. Non-Cryst. Solids 71 (1985) 203–217.
[63] G.N. Greaves, S. Sen, Inorganic glasses, glass-forming liquids and amorphizing solids, Adv. Phys. 56 (2007) 1–166.
[64] P. Yunker, Z. Zhang, K.B. Aptowicz, A.G. Yodh, Irreversible rearrangements, correlated domains, and local structure in aging glasses, Phys. Rev. Lett. 103 (2009) 115701.
[65] D. Hülsenberg, A. Harnisch, A. Bismarck, Microstructuring of Glasses, Springer-Verlag, Berlin Heidelberg, 2008.
[66] Ye.A. Golubev, Scanning probe microscopy in researches of micro- and nanostructure in noncristalline geomaterials, Microsc. Microanal. 9 (2003) 304–305.
[67] Ye.A. Golubev, Supermolecular nanostructurization in natural colloids: scanning probe microscopy data, J. Cryst. Growth 275 (1–2) (2005) e2357–e2360.
[68] K. Shimoda, M. Okuno, Y. Syono, M. Kikuchi, K. Fukuoka, M. Koyano, S. Katayama, Structural evolutions of an obsidian and its fused glass by shock-wave compression, Phys. Chem. Miner. 31 (2004) 532–542, https://doi.org/10.1007/s00269-004-0408-9.
[69] D.M. Zirl, S.H. Garofalini, Structure of sodium aluminosilicate glass surfaces, J. Am. Ceram. Soc. 75 (191) (1992) 2353–2362.
[70] Y. Xiang, J. Du, M.M. Smedskjaer, J.C. Mauro, Structure and properties of sodium aluminosilicate glasses from molecular dynamics Simulations, J. Chem. Phys. 139 (2013) 044507, , https://doi.org/10.1063/1.4816378.
[71] Y. Yu, M. Wang, N.M. Anoop Krishnan, M.M. Smedskjaer, K.D. Vargheese, J.C. Mauro, M. Balonise, M. Bauchy, Hardness of silicate glasses: atomic-scale origin of the mixed modifier effect, J. Non-Cryst. Solids 489 (2018) 16–21.
[72] B. Bauluz, D.R. Peacor, C.J. Hollis, TEM study of meteorite impact glass at New Zealand cretaceous tertiary sites: evidence for multiple impacts or disorientation during global circulation? Earth Planet. Sci. Lett. 219 (2004) 209–219.
[73] T.G. Shumilova, V.P. Lutoev, S.I. Isaenko, N.S. Kovalchuk, B.A. Makeev, A.Yu. Lysiuk, A.A. Zubov, K. Ernstson, Spectroscopic features of ultrahigh-pressure impact glasses of the kara astrobleme, Sci. Rep. 8 (1) (2018), https://doi.org/10.1038/s41598-018-25037-z.
[74] G.R. Osinski, Impact glasses in fallout suevites from the Ries impact structure, Germany: an analytical SEM study, Meteorit. Planet. Sci. 38 (2003) 1641–1667.